Available online at www.scholarsresearchlibrary.com

Scholars Research Library

Der Pharmacia Lettre, 2016, 8 (4):65-76
(http://scholarsresearchlibrary.com/archive.html)

ISSN 0975-5071
USA CODEN: DPLEB4

Corrosion control of carbon steel in hydrochloric acid by Sulfaguandine: Weight loss, electrochemical and theoretical studies

M. Saadouni[1], M. Larouj[2], R. Salghi[3*], H. Lgaz[2,3], S. Jodeh[4,*], M. Zougagh[5,6] and A. Souizi[1]

[1]*Laboratory of Organic, Organometallic and Theoretical Chemistry, Faculty of Science, Ibn Tofaïl University, 14000 Kenitra, Morocco*
[2]*Laboratory separation processes, Faculty of Science, University IbnTofail PO Box 242, Kenitra, Morocco*
[3]*Laboratory of Applied Chemistry and Environment, ENSA, Université Ibn Zohr,PO Box 1136, 80000 Agadir, Morocco*
[4]*Department of Chemistry, An-Najah National University, P. O. Box 7, Nablus, Palestine*
[5]*Regional Institute for Applied Chemistry Research, IRICA, E-13004, Ciudad Real, Spain*
[6]*Castilla-La Mancha Science and Technology Park, E-02006, Albacete, Spain*

ABSTRACT

*In this work, we studied the effect of inhibition of Sulfaguandine**(SFG)** against corrosion of the carbon steel in hydrochloric acid 1.0M HCl. For this, we used the weight loss measurements and electrochemical methods such as potentiodynamic polarization and electrochemical impedance spectroscopy (EIS). Results obtained revealed that **SFG** performed excellently as a corrosion inhibitor for carbon steel in hydrochloric acid solution. Inhibition efficiency increases with increase in concentration of **SFG**. The efficiency reaches a maximum value of 95.71% at 5×10^{-3}M. Electrochemical methods show that it acts as mixed-type inhibitor with predominant cathodic action. The **SFG** admits as the Langmuir adsorption. The thermodynamic activation parameters for the corrosion reaction were calculated and discussed in relation to the stability of the protective inhibitor layer. Attempt to correlate the molecular structure to quantum chemical indices was made using density functional theory (DFT).*

Keywords: Sulfaguanidine inhibitor, Carbon steel, 1.0M HCl, EIS, Polarization, DFT.

INTRODUCTION

Corrosion is a fundamental process playing an important role in economics and safety, particularly for metals and alloys. Steel has found wide application in a broad spectrum of industries and machinery; however its tendency to corrosion. The corrosion of steel is a fundamental academic and industrial concern that has received a considerable amount of attention [1-7].

Among several methods used in combating corrosion problems, the use of chemical inhibitors remains the most cost effective and practical method. Therefore, the development of corrosion inhibitors based on organic compounds containing nitrogen, sulphur and oxygen atoms functional groups, aromaticity, the possible steric effects and electronic density of donorsare of growing interest in the field of corrosion and industrial chemistry as corrosion poses serious problem to the service lifetime of alloys used in industry [8-17].

The purpose of this paper is to evaluate the corrosion of carbon steel in the absence and the presence of (**SFG**) in 1.0 M HCl. The inhibition effect of **SFG** on steel in 1.0 M HCl is studied for the first time by weight loss, potentiodynamic polarisation curves and electrochemical impedance spectroscopy (EIS) methods. Also the relationship between quantum chemical calculations and experimental inhibition efficiencies of the inhibitor was discussed. The structure of **SFG** is shown in Fig. 1

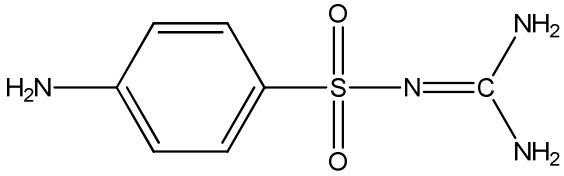

Figure1. Molecular structure of Sulfaguandine (SFG)

MATERIALS AND METHODS

Materials

The steel used in this study is a carbon steel (Euronorm: C35E carbon steel and US specification: SAE 1035) with a chemical composition (in wt%) of 0.370 % C, 0.230 % Si, 0.680 % Mn, 0.016 % S, 0.077 % Cr, 0.011 % Ti, 0.059 % Ni, 0.009 % Co, 0.160 % Cu and the remainder iron (Fe). The carbon steel samples were pre-treated prior to the experiments by grinding with emery paper SiC (120, 600 and 1200); rinsed with distilled water, degreased in acetone in an ultrasonic bath immersion for 5 min, washed again with bidistilled water and then dried at room temperature before use. The acid solutions (1.0 M HCl) were prepared by dilution of an analytical reagent grade 37 % HCl with double-distilled water. The concentration range of Sulfaguandine employed was 5.10^{-3}M to 1.10^{-4} M.

Measurements

Weight loss measurements

The gravimetric measurements were carried out at definite time interval of 6 h at room temperature using an analytical balance (precision ± 0.1 mg). The carbon steel specimens used have a rectangular form (length = 1.6 cm, width = 1.6 cm, thickness = 0.07 cm). Gravimetric experiments were carried out in a double glass cell equipped with a thermostated cooling condenser containing 80 mL of non-de-aerated test solution. After immersion period, the steel specimens were withdrawn, carefully rinsed with bidistilled water, ultrasonic cleaning in acetone, dried at room temperature and then weighted. Triplicate experiments were performed in each case and the mean value of the weight loss was calculated.

Electrochemical measurements

Electrochemical experiments were conducted using impedance equipment (Tacussel-Radiometer PGZ 100) and controlled with Tacussel corrosion analysis software model Voltamaster 4. A conventional three-electrode cylindrical Pyrex glass cell was used. The temperature is thermostatically controlled. The working electrode was carbon steel with the surface area of 1 cm^2. A saturated calomel electrode (SCE) was used as a reference. All potentials were given with reference to this electrode. The counter electrode was a platinum plate of surface area of 1 cm^2. A saturated calomel electrode (SCE) was used as the reference; a platinum electrode was used as the counter-electrode. All potentials are reported *vs*. SCE. All electrochemical tests have been performed in aerated solutions at 303K.

For polarization curves, the working electrode was immersed in a test solution during 30 min until a steady state open circuit potential (E_{ocp}) was obtained. The polarization curve was recorded by polarization from -800 to -200 mV/ SCE with a scan rate of 1 mV s^{-1}. AC impedance measurements were carried-out in the frequency range of 100 kHz to 10 mHz, with 10 points per decade, at the rest potential, after 30 min of acid immersion, by applying 10 mV ac voltage peak-to-peak. Nyquist plots were made from these experiments. The best semicircle can be fit through the data points in the Nyquist plot using a non-linear least square fit so as to give the intersections with the *x*-axis.

Molecular Modelling

Quantum chemical method is usually used to explore the relationship between the inhibitor molecular properties and its corrosion inhibition efficiency [18]. The properties include orbital energy, charge density and combined energy, etc. [19].Past studies have investigated the correlation between the inhibitor molecular structure and its efficiency, but much less attention has been paid to simulate the adsorption mode of the inhibitor and the metal. Quantum chemical calculations were performed using DFT (density functional theory) with the Beck's three parameter exchange functional along with the Lee-Yang-Parr non local correlation functional (B3LYP) [20-22] with 6-31G (d,p) basis set is implemented in Gaussian 03 program package [23].

This approach is shown to yield favorable geometries for a wide variety of systems. The following quantum chemical parameters were calculated from the obtained optimized molecular structure: the dipole moment (μ), the energy of the highest occupied molecular orbital (E_{HOMO}), the energy of the lowest unoccupied molecular orbital (E_{LUMO}), the energy band gap ($\Delta Egap = E_{HOMO} - E_{LUMO}$), the electron affinity (A), the ionization potential (I) and the number of transferred electrons (ΔN).

According to Koopman's theorem [24] the ionization potential (IE) and electron affinity (EA) of the inhibitors are calculated using the following equations.

$$IE = -E_{HOMO} \quad (1)$$

$$AE = -E_{LUMO} \quad (2)$$

Thus, the values of the electronegativity (χ) and the chemical hardness (η) according to Pearson, operational and approximate definitions can be evaluated using the following relations [25]:

$$\chi = \frac{I + A}{2} \quad (3)$$

$$\eta = \frac{I - A}{2} \quad (4)$$

The number of transferred electrons (ΔN) was also calculated depending on the quantum chemical method [26, 27] by using the equation:

$$\Delta N = \frac{\chi_{Fe} - \chi_{inh}}{2(\eta_{Fe} + \eta_{inh})} \quad (5)$$

Where χ_{Fe} and χ_{inh} denote the absolute electronegativity of iron and inhibitor molecule η_{Fe} and η_{inh} denote the absolute hardness of iron and the inhibitor molecule respectively. In this study, we use the theoretical value of χ_{Fe} =7.0 eV mol^{-1} and η_{Fe} = 0 eV mol^{-1}, for calculating the number of electron transferred.

RESULTS AND DISCUSSION

Effect of concentration

Polarization curves

Polarization measurements have been carried out in order to gain knowledge concerning the kinetics of the anodic and cathodic reactions. Polarization curves of the carbon steel in 1.0M HCl solutions without and with addition of different concentrations of **SFG** at 303 K are shown in Figure2.The anodic and cathodic current–potential curves are extrapolated up to their intersection at a point where corrosion current density (I_{corr}) and corrosion potential (E_{corr}) are obtained. Table1shows the electrochemical parameters (I_{corr}, E_{corr} and b_c) obtained from Tafel plots for the carbon steel electrode in 1.0 M HCl solution without and with different concentrations of **SFG**. The I_{corr} values were used to calculate the inhibition efficiency, η_{PDP} (%) (Listed in Table1), using the following equation:

$$\eta_{PDP}(\%) = \frac{I_{corr} - I_{corr(i)}}{I_{corr}} \times 100 \quad (6)$$

Where I_{corr} and $I_{corr(i)}$ are the corrosion current densities for carbon steel electrode in the uninhibited and inhibited solutions, respectively.

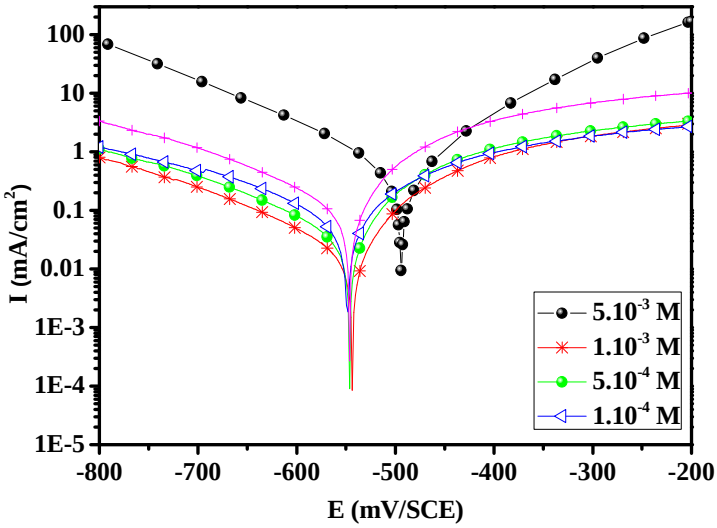

Figure2. Polarisation curves of carbon steel in 1.0 M HCl for various concentrations of SFG at 303K

From this figure, it can be seen that with the increase of **SFG** concentrations, both anodic and cathodic currents were inhibited. This result shows that the addition of **SFG** inhibitor reduces anodic dissolution and also retards the hydrogen evolution reaction. The Tafel lines in Figure2 were almost parallel upon increasing the inhibitor concentrations. It suggested that the inhibitor acted by simple blocking of the mild steel surface [28]. In other words, the inhibitor decreased the surface area for corrosion and did not change the mechanism of either mild steel dissolution or hydrogen evolution reaction.

Table1. Polarization data of carbon steel in 1.0 M HCl without and with various concentrations of SFG at 303 K

Inhibitor	Conc (M)	$-E_{corr}$ (mV/SCE)	$-\beta c$ (mV dec^{-1})	I_{corr} (µA cm^{-2})	η_{Tafel} (%)	Θ
Blank	-	496.0	162	564.0	-	-
SFG	5.10^{-3}	546	164	24.18	95.71	0.957
	1.10^{-3}	544	163	56.37	90.00	0.900
	5.10^{-4}	545	160	105.87	81.23	0.812
	1.10^{-4}	549	172	172.13	69.48	0.694

Table1 showed that the largest displacement of the corrosion potential (E_{corr}) was about 53 mV. But only when the change in E_{corr} value is no less than 85 mV, it can be recognised as a classification evidence of a compound as an anodic or a cathodic-type inhibitor [29]. Therefore, it can be understood from the E_{corr} variation that the studied compounds might act as mixed-type inhibitor, and its η_{Tafel} % increased with the concentration. At the concentration of 5.10^{-3}mol/L, the studied compound had good inhibition efficiency about95.71% and acted as excellent hydrochloride acid inhibitor. The results indicated that the increase in inhibitor efficiency with concentration might be attributed to the formation of a barrier film, which prevents the acid medium that attacks the metal surface due to the adsorption of these compounds on the mild steel surface.

Electrochemical Impedance Spectroscopy

Figure3 shows the Nyquist diagrams of carbon steel in 1.0 M HCl solutions containing different concentrations of **SFG** at 308K. All the impedance spectra exhibit one single depressed semicircle. The diameter of semicircle increases with the increase of **SFG** concentration and the decrease of the temperature. The semicircular appearance shows that the corrosion of carbon steel is controlled by the charge transfer and the presence of **SFG** does not change the mechanism of carbon steel dissolution [30]. In addition, these Nyquist diagrams are not perfect semicircles. The deviation of semicircles from perfect circular shape is often referred to as the frequency dispersion of interfacial impedance [30, 31]. This behavior is usually attributed to the inhomogeneity of the metal surface arising from surface roughness or interfacial phenomena [32, 33] which is typical for solid metal electrodes. Generally, when a non-ideal frequency response is present, it is commonly accepted to employ the distributed circuit elements in the equivalent circuits. What is most widely used is the constant phase element (CPE), which has a non-integer power dependence on the frequency [34, 35]. Thus, the equivalent circuit depicted in Figure4 is employed to analyze the impedance spectra, where R_s represents the solution resistance, R_t denotes the charge-transfer resistance,

and a CPE instead of a pure capacitor represents the interfacial capacitance. Excellent fit with this model was obtained for all experimental data. The impedance of a CPE is described by the expression[36]:

$$Z_{CPE} = \frac{1}{Q(j\omega)^n} \quad (7)$$

Where Q is the CPE constant (in $\Omega^{-1}S^n\ cm^{-2}$), ω is the angular frequency (in rad s^{-1}), $j^2 = -1$ is the imaginary number and n is a CPE exponent which can be used as a gauge for the heterogeneity or roughness of the surface.

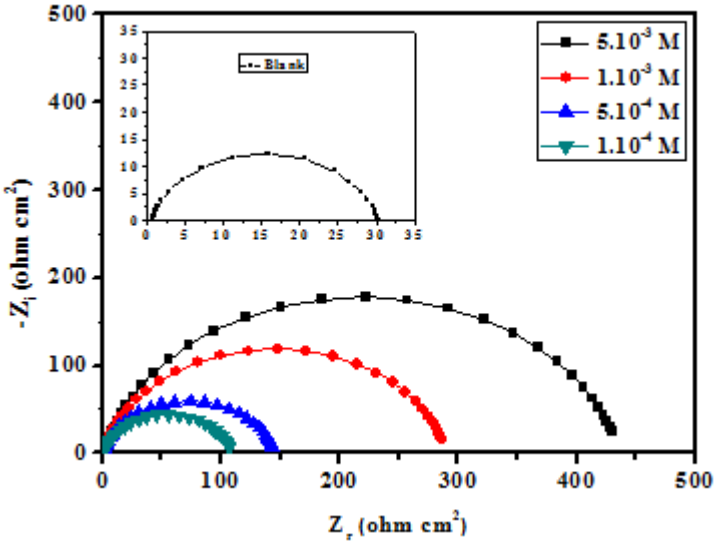

Figure 3.Nyquist diagrams for carbon steel in 1.0 M HCl containing different concentrations of SFG at 303 K

In addition, the double layer capacitances, C_{dl}, for a circuit including a CPE were calculated by using the following equation[37]:

$$C_{dl} = \left(Q.\ R_{ct}^{\ 1-n}\right)^{1/n} \quad (8)$$

The values of percentage inhibition efficiency η_{EIS} were calculated from the values of R_{ct} according to the following equation [38]:

$$\eta_{EIS}(\%) = \left(\frac{R_{ct} - R^{\circ}_{ct}}{R_{ct}}\right) \times 100 \quad (9)$$

Where R°_{ct} and R_{ct} are the charge transfer resistances without and with various concentrations of inhibitors respectively. Several impedance parameters such as R_{ct}, C_{dl}, n, θ, Q and η_{EIS}(%) were derived using above equivalent circuit shown in Figure4 and are given in Table2.

Table2. Impedance parameters for corrosion of carbon steel in 1.0 M HCl in the absence and presence of different concentrations of SFG at 303 K

Inhibitor	Conc (g/L)	R_{ct} ($\Omega\ cm^2$)	n	$Q\times10^{-4}$ ($s^n\ \Omega^{-1}cm^{-2}$)	C_{dl} ($\mu F\ cm^{-2}$)	η_{EIS}(%)	Θ
Blank	-	29 .35	0.91	1.7610	91.63	-	-
SFG	5.10^{-3}	434.1	0.87	0.2037	10	93.24	0.932
	1.10^{-3}	289.4	0.87	0.3055	15	89.86	0.898
	5.10^{-4}	144.7	0.89	0.6111	34	79.72	0.797
	1.10^{-4}	108.5	0.83	1.2435	51	72.95	0.729

As is seen from Table2, the C_{dl} values decrease with the increase of **SFG** concentration, which suggests that **SFG** functions by adsorption on the carbon steel surface. It is inferred that the **SFG** molecules gradually replace the water molecules by adsorption at the metal/solution interface, which leads to the formation of a protective film on the carbon steel surface and thus decreases the extent of the dissolution reaction [31]. Moreover, the increase of **SFG** concentration leads to the increase of R_{ct} and η_{EIS}% values. The corrosion inhibition efficiency reaches more than 93.24% in the presence of 5.10^{-3} M **SFG**. The change trend of η_{EIS} % can be related to the surface coverage of

SFGon carbon steel, namely, with an increase in **SFG** concentration, its surface coverage on carbon steel also increases. The high η_{EIS}% (and surface coverage) at the low concentration of **SFG** leads to the assumption that the adsorption of **SFG** molecules occurs not on the whole surface of carbon steel, but only on the active sites.

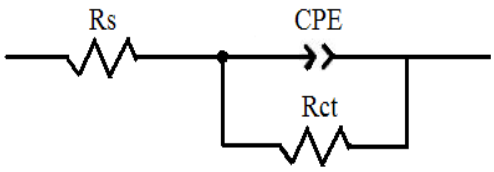

Figure4. Equivalent electrical circuit corresponding to the corrosion process on the carbon steel in hydrochloric acid

Weight loss measurements

The effect of addition of **SFG** tested at different concentrations on the corrosion of carbon steel in 1.0 M HCl solution was studied by weight loss measurements at 303 K after 6 h of immersion period. From the values of corrosion rate in the absence (C_R) and presence ($C_{R\ (inh)}$) of inhibitor, the inhibition efficiency, η_{wL} (%), was determined using the following equation:

$$\eta_{wL}(\%) = \frac{C_R - C_{R(inh)}}{C_R} \times 100 \qquad (10)$$

It is obvious from the Table3that the **SFG** inhibit the corrosion of carbon steel in 1.0 M HCl solution at all concentrations used in this study and the corrosion rate (C_R) is seen to decrease continuously with increasing additive concentration at 303 K. Indeed, corrosion rate values of carbon steel decrease when the inhibitor concentration increases while η_{wL} (%)values of **SFG** increase with the increase of the concentration, the maximum η_{wL} (%)of 94.36% is achieved at 5.10^{-3}M.

Table3. Corrosion parameters obtained from weight loss measurements for carbon steel in 1.0 M HCl containing various concentration of SFG at 303 K

Inhibitor	Concentration (M)	C_R (mg cm^{-2} h^{-1})	η_{wL} (%)	Θ
Blank	-	1.135	-	-
SFG	5.10^{-3}	0.064	94.36	0.943
	1.10^{-3}	0.127	88.78	0.887
	5.10^{-4}	0.216	80.93	0.809
	1.10^{-4}	0.304	73.18	0.731

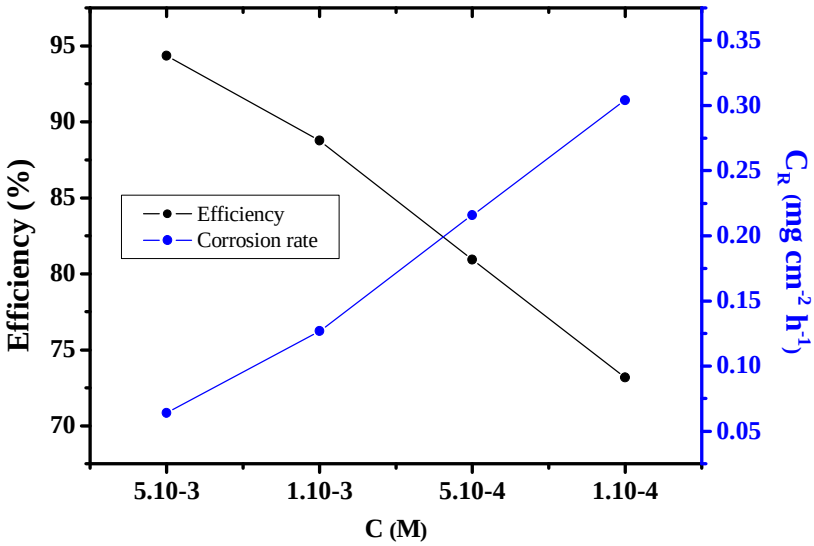

Figure 5. Relationship between the corrosion rate, the inhibition efficiency and SFG concentrations for steel after 6 h immersion in 1.0 M HCl at 303 K

Effect of temperature and thermodynamic activation parameters

In general, the effect of temperature on the inhibited acid–metal reaction is highly complex, because many changes occur on the metal surface such as rapid etching and desorption of inhibitors and the inhibitor itself may undergo decomposition or rearrangement [39]. In order to calculate the activation parameters and evaluate the mechanism of inhibition, Weight loss measurementswere performed for carbon steel in 1.0 M HCl in the absence and presence of 5.10^{-3}M **SFG** inhibitor in the temperature range of 303-333 K. The effect of temperature on the corrosion rate of carbon steel in 1.0 M HCl over the temperature range (303 to 333K) (see Table4) in the absence and presence of different concentrations of the investigated compounds has been studied. The inhibition efficiency is found to decrease with increasing the temperature; this indicated that, this compound is physically adsorbed on the carbon steel surfaces.

Table4. C_R and η_w % obtained from weight loss measurements of mild steel in 1.0 M HCl containing 5.10^{-3}M of SFG at different temperatures

Inhibitors	Temperature (K)	C_R (mg cm^{-2} h^{-1})	η_w (%)	Θ
Blank	303	1.135	-	-
	313	2.466	-	-
	323	5.032	-	-
	333	10.029	-	-
SFG	303	0.062	**94.54**	0.945
	313	0.284	**88.48**	0.884
	323	1.137	**77.40**	0.774
	333	3.781	**62.29**	0.622

The dependence of corrosion rate at temperature can be expressed by Arrhenius equation and transition state equation:[40]

$$C_R = k\, exp\left(\frac{-E_a}{RT}\right) \tag{11}$$

$$C_R = \frac{RT}{Nh}\, exp\left(\frac{\Delta S_a}{R}\right) exp\left(-\frac{\Delta H_a}{RT}\right) \tag{12}$$

Where C_R is the corrosion rate, R the gas constant, T the absolute temperature, k the pre-exponential factor, h is the Planck's constant (6.626176×10^{-34} Js), N is the Avogadro's number, ΔH_a the enthalpy of activation, and ΔS_a entropy of activation. The apparent activation energy for a 5.10^{-3}M of concentration of the inhibitor can be calculated by linear regression between Ln (C_R) and 1/T; the results were shown in Table5.

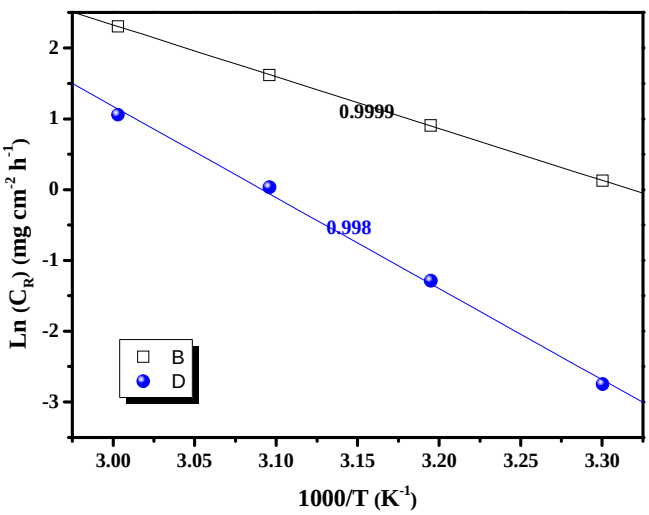

Figure6. Arrhenius plots for MS in 1.0 M HCl in the absence and presence of 1mM of SFG at different temperatures

A plot shown in Figure6, of corrosion rate obtained by weight loss measurement versus 1/T gave straight line. The value of the E_a obtained from the slope equals to the ($-E_a/R$).It is evident from the Table5 that the activation energy increased on addition of **SFG** in comparison to the uninhibited solution. The increase in the apparent activation energy value interpreted as the decrease in the inhibition efficiency with the increase in the temperature. This leads to the increase in corrosion rate due to the greater area of metal that is exposed towards the corrosive environment [41].

A plot of Ln (C_R/T) versus 1/T is shown in Figure 7. Straight lines were obtained with slope ($-\Delta H_a/R$) and intercept of [Ln(R/Nh) + ($\Delta S_a/R$)], from which ΔH_a and ΔS_a were calculated and listed in Table5. It is clear from the Table5 that the entropy of activation increased in the presence of inhibitor in comparison to the uninhibited sample. The increase in the activation entropy in presence of inhibitor indicates the increase in the disorderliness on going from reactant to activated complex. It is evident from the table that the value of ΔH_a increased in the presence of inhibitor than in the uninhibited solution indicating the higher inhibitive efficiency. This may be attributed to the presence of an energy barrier for the reaction, hence, the process of adsorption of inhibitor leads to rise in enthalpy of the corrosion process.

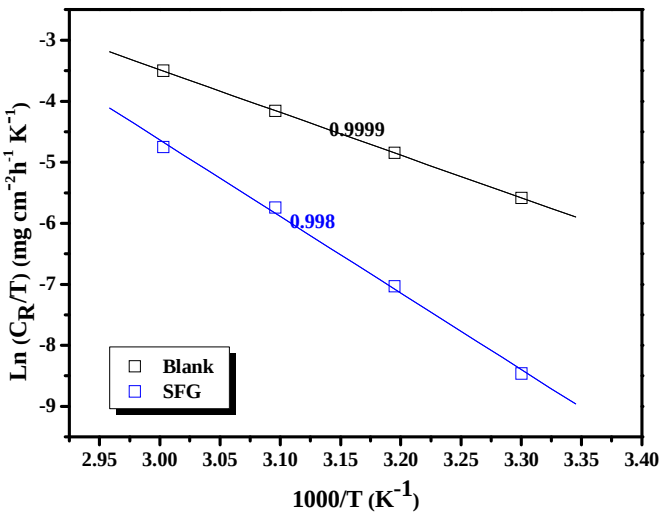

Figure 7.Transition state plots for the inhibition of corrosion of mild steel in 1.0 M HCl in the absence and presence of 5mM of SFG at different temperatures

Table5. Activation parameters for mild steel corrosion in 1.0M HCl in the absence and presence of 5 mM SFG inhibitor at different temperatures

Inhibitor	E_a (kJ/mol)	ΔH_a (kJ/mol)	ΔS_a (J mol^{-1} K^{-1})	$E_a - \Delta H_a$
Blank	60.79	58.16	-51.84	2.63
5mM **SFG**	106.94	104.3	77.04	2.64

Adsorption isotherm and thermodynamic parameters

It is well recognized that the first step in inhibition of metallic corrosion is the adsorption of organic inhibitor molecules at the metal/solution interface and that the adsorption depends on the molecules chemical composition, the temperature and the electrochemical potential at the metal/solution interface. In fact, the solvent H_2O molecules could also adsorb at metal/solution interface. So the adsorption of organic inhibitor molecules from the aqueous solution can be regarded as a quasi-substitution process between the organic compounds in the aqueous phase [$Org_{(sol)}$] and water molecules at the electrode surface [$H_2O_{(ads)}$] [42]:

$$Org_{(sol)} + nH_2O_{(ads)} \rightarrow Org_{(ads)} + nH_2O_{(sol)}$$

Where (n) is the size ratio, that is, the number of water molecules replaced by one organic inhibitor. Basic information on the interaction between they inhibitor and the steel surface can be provided by the adsorption isotherm. In order to obtain the isotherm, the linear relation between degree of surface coverage (θ) values ($\theta = \eta_{WL}$ % / 100) and inhibitor concentration (C) must be found. Attempts were made to fit the θ values to various isotherms including Langmuir, Temkin and Frumkin. By far the best fit is obtained with the Langmuir isotherm. This model has also been used for other inhibitor systems [43,44].According to this isotherm, θ is related to C by:

Langmuir: $$\frac{C}{\theta} = \frac{1}{K} + C \quad (13)$$

Frumkin: $$Ln\left[\frac{(1-\theta)C}{\theta}\right] = LnK + g\theta \quad (14)$$

Temkin: $$Ln\left(\frac{\theta}{C}\right) = LnK - g\theta \quad (15)$$

θ is the surface coverage, K is the adsorption-desorption equilibrium constant, Cis the concentration of inhibitor and g is the adsorbate parameter.

Figure8 shows the plots of C /θ versus C and the expected linear relationship is obtained for this compound. The strong correlation (R^2 = 0.9999 for the compound **SFG**) confirm the validity of this approach.

The thermodynamic parameters from the Langmuir adsorption isotherm are listed in Table6, together with the value of the Gibbs free energy of adsorption ΔG°_{ads} calculated from the equation:

$$\Delta G^{\circ}_{ads} = -RTLn(55.5K_{ads}) \quad (16)$$

Where R is the universal gas constant, the thermodynamic temperature and the value of 55.5 is the concentration of water in the solution [45].

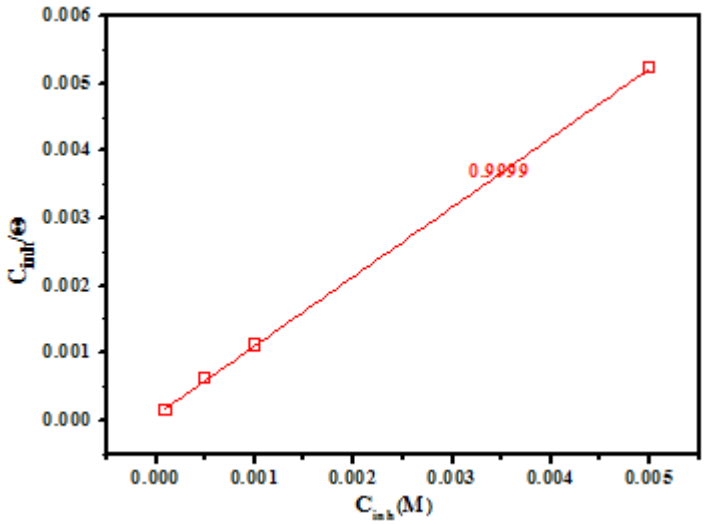

Figure 8.Langmuir adsorption of SFG inhibitor on the mild steel surface in 1.0 M HCl solution at 303K

Table6. Adsorption parameters of SFG for mild steel corrosion in 1.0M HCl at 303 K

Inhibitor	Slope	$K_{ads}(M^{-1})$	ΔG°_{ads} (kJ/mol)
SFG	1.03	13794.26	-34.11

Generally, the energy values of -20 kJ mol-1or less negative are associated with an electrostatic interaction between charged molecules and charged metal surface, physisorption; those of -40 kJ mol-1 or more negative involve charge sharing or transfer from the inhibitor molecules to the metal surface to form a coordinate covalent bond, chemisorption [46,47]. The value of the standard free energy of adsorption $\Delta G°_{ads}$ listed in Table6, since it is between the values of -40 kJ mol^{-1} and -20 kJ mol^{-1}, allows us to suggest that the adsorption of our inhibitors has two types of interactions: chemisorption and physisorption [48].

Theoretical parameters predicating

Quantum chemical calculations are utilized to ascertain whether there is a clear relationship between the molecular structures of inhibitor and its inhibition effect. The structure parameters and adsorptive performance of the

synthesized inhibitor are used to elucidate the inhibition mechanism in the present work. The equilibrium geometry structures and the frontier molecule orbital (FOM) density distributions of the molecule are shown in Fig. 9and the quantum theoretical parameters are listed in Table 7.

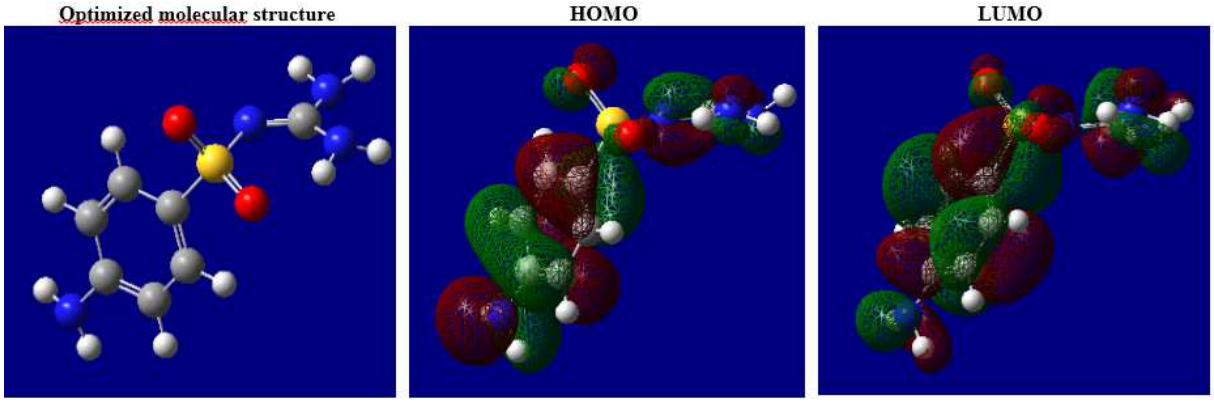

Figure10.Optimized structure and frontier molecular orbital diagrams of SFG by B3LYP/6-31G (d,p)

Table6. Quantum chemical parameters for SFG calculated using B3LYP/6-31G (d,p)

Molecular parameters	**SFG**
E_{HOMO} (eV)	-5.95439855
E_{LUMO} (eV)	-0.55946638
ΔE_{gap} (eV)	5.39493216
μ (debye)	7.1137
I (eV)	5.95439855
A (eV)	0.55946638
χ (eV)	3.25693247
η (eV)	2.69746608
ω	14.3068329
ΔN	0.69381179
TE (a.u)	-1040.56

Analysis of Fig. 9shows that the distribution of energies HOMO and LUMO are distributed over the entire molecule, consequently this is the favorite's sites for interaction with the metal surface. These results suggest that the nitrogen and oxygen atoms are the probable reactive sites for adsorption of inhibitor on the metal surface.

E_{HOMO} is often associated with the electron-donating ability of a molecule and its high value (-5.95439855 eV) is likely to indicate a tendency to donate electrons to appropriate low-energy acceptor states. Increasing values of the E_{HOMO} facilitate adsorption (and therefore inhibition) by influencing the transport process through the adsorbed layer. E_{LUMO} indicates the ability of the molecule to accept electrons; hence these are the acceptor states. The lower the value (-0.55946638 eV) of E_{LUMO}, the more probable it is that the molecule would accept electrons [26]. For the dipole moment (μ), higher value (7.1137 D), of dipole moment will favor a strong interaction of inhibitor molecules to the metal surface.
In addition, the electro negativity parameter (χ) is related to the chemical potential, and higher value of (χ) indicates better.

Using Eq. (4), the value of electron-donating ability (ΔN) was calculated and its value is given in Table 1. If ΔN < 3.6 (electron), the inhibition efficiency increases with increasing value of ΔN, while it decreased if ΔN > 3.6 (electron) [27, 28]. In present contribution, SFG is the donor of electrons, and the iron surface atom was the acceptor. The SFG was bound to the mild steel surface, and thus formed inhibition adsorption layer against corrosion at carbon steel/hydrochloric acid solution interface.

CONCLUSION

From the above results and discussion, the following conclusions are drawn:

- The results showed that inhibitor Sulfaguandine(SFG) have excellent inhibition efficiency for the corrosion of Carbon steel in 1.0 M HCl.
- The inhibition efficiency increases with concentration compound.
- The potentiodynamic polarization curves indicated that Sulfaguandine act as mixed type of inhibitor.

➢ The Sulfaguandine molecule follows Langmuir adsorption isotherm for the adsorption on metal surface in 1.0 M HCl solution.
➢ The impedance results indicate that the value of polarization resistance increased and double layer capacitance decreased. This result can be attributed to the increase of thickness of electrical double layer.
➢ Inhibition efficiency of this inhibitor decreases with increase in temperature and further it leads to an increase in activation energy.
➢ Quantum chemical calculations showed a good correlation between quantum chemical parameters for the investigated compound and its inhibition efficiency for the corrosion process in agreement with experimental results.

Acknowledgment
The authors would like to thank the Palestinian Ministry of Higher Education for their support. The support given through an "INCRECYT" research contract to M. Zougagh is also acknowledged.

REFERENCES

[1] Solmaz R, Kardaş G, Yazici B, Erbil M, *Colloids Surf.* A,**2008**, 7, 312.
[2] Prajila M, Sam J, Bincy J, Abraham J, *J. Mater. Environ. Sci*,**2012**, 3, 1045.
[3] Naik U J,Panchal V A, Patel A S, Shah N K, *J. Mater. Environ Sci*,**2012**, 3, 935.
[4] M Larouj, M Belayachi, H Zarrok, A Zarrouk, A Guenbour, M Ebn Touhami, A Shaim, S Boukhriss, H Oudda, B Hammouti, *Der Pharma Chemica*, **2014**, 6(3), 373-384.
[5] M Larouj, H Lgaz, HZarrok, H Serrar, H Zarrok, H Bourazmi, A Zarrouk, A Elmidaoui, A Guenbour, S Boukhris and H Oudda.*J. Mater. Environ Sci*,**2015**, 6 (11), 3251-3267.
[6] M Larouj, M Belkhaouda, H Lgaz, R Salghi, S Jodeh, S Samhan, H Serrar, S Boukhris, M Zougagh and H Oudda, *Der Pharma Chemica*, **2016**, 8(2), 114-133.
[7] H Lgaz, O Benali, R Salghi, S Jodeh, M Larouj, O Hamed, MMessali, SSamhan, M Zougagh and H Oudda. *Der Pharma Chemica*, **2016**, 8(2), 172-190.
[8] Ben Hmamou D, Salghi R, Zarrouk A, Zarrok H, Hammouti B, Al-Deyab S S, Bouachrine M, Chakir A, Zougagh M, *Int. J. Electrochem. Sci*,**2012**, 7, 5716.
[9] L Afia, MLarouj, H Lgaz, R Salghi, S Jodeh, S Samhan and M Zougagh, *Der Pharma Chemica*, **2016**, 8(2), 22-35.
[10] B El Makrini, M Larouj, H Lgaz, R Salghi, A Salman, M Belkhaouda, S Jodeh, M Zougagh and H Oudda. *Der Pharma Chemica*, **2016**, 8(2), 227-237.
[11] B El Makrini, H Lgaz, M Larouj, R Salghi, A Rasem Hasan, M Belkhaouda, S Jodeh, M Zougagh and H Oudda, *Der Pharma Chemica*, **2016**, 8(2), 256-268.
[12] Ben Hmamou D, Salghi R, Zarrouk A, Zarrok H, Al-Deyab S S, Benali O, Hammouti B *Int. J. Electrochem. Sci*,**2012**, 7, 8988.
[13] H Lgaz, Y ELaoufir, Y Ramli, M Larouj, H Zarrok, R Salghi, A Zarrouk, A Elmidaoui, A Guenbour, EL M Essassi and H Oudda, *Der Pharma Chemica*, **2015**, 7(6), 36-45.
[14] H Lgaz, M Belkhaouda, M Larouj, R Salghi, S Jodeh, I Warad, H Oudda. A Chetouani, *Mor. J. Chem*, **2016**, 4(1), 101- 111
[15] M Belayachi, H Zarrok, M Larouj, A Zarrouk, H Bourazmi, A Guenbour, B Hammouti, S Boukhriss, H Oudda, *Phys. Chem. News*,**2014**, 74, 85-93.
[16] F Bentiss, M Lagrenee, M Traisnel, *Corrosion*, **2000**, 56, 733.
[17] F Bentiss, M Traisnel, M Lagrenee, *J. Appl. Electrochem*,**2001**, 31, 41.
[18] N Khalil, *Electrochim. Acta*,**2003**, 48, 2635.
[19] M Ozcan, I Dehri, M Erbil, *Appl. Surf. Sci*,**2004**, 236, 155.
[20] A D Becke, *J. Chem. Phys*,**1992**, 96, 9489.
[21] A D Becke, *J. Chem. Phys*,**1993**, 98, 1372.
[22] C Lee, W Yang, R G Parr, *Phys Rev*. B,**1988**, 37, 785.
[23] M J Frisch et al, GAUSSIAN 03, Revision B 03, Gaussian, Inc, Wallingford, CT, **2004**.
[24] R G Pearson, *Inorg. Chem*, **1988**, 27,734.
[25] V S Sastri, J R Perumareddi, *Corrosion* (NACE) **1997**, 53, 617.
[26] I Lukovits, E Kalman, F Zucchi, *Corrosion* (NACE) **2001**, 57, 3.
[27] Y Abboud, A Abourriche, T Saffaj, M Berrada, *Appl. Surf. Sci*,**2006**, 252, 8178
[28] H Ashassi-Sorkhabi, M R Majidi, K Seyyedi, *Appl. Surf. Sci*,**2004**, 225, 176
[29] H Shih, F Mansfeld, *Corros. Sci*,**1989**, 29, 1235.
[30] S Martinez, M Metikoš-Hukovic, *J. Appl. Electrochem*,**2003**, 33, 1137.
[31] F Bentiss, M Lebrini, H Vezin, F Chai, M Traisnel, M Lagrené, *Corros. Sci*,**2009**, 51, 2165.
[32] M Kissi, M Bouklah, B Hammouti, M Benkaddour, *Appl. Surf. Sci*,**2006**, 252, 4190.
[33] S F Mertens, C Xhoffer, B C De Cooman, E Temmerman, *Corrosion*,**1997**, 53, 381.

[34] Y P Khodyrev, E S Batyeva, E K Badeeva, E V Platova, L Tiwari, O G Sinyashin, *Corros. Sci*,**2011**, 53, 976.
[35] C B Verma, M A Quraishi, et A Singh, J. *Taiwan Inst. Chem. Eng*, **2015**, 49, 229-239.
[36] C B Verma, M A Quraishi, et A Singh, J. *Taiwan Inst. Chem. Eng*, **2015**, 49, 229.
[37] X H Li, S D Deng, H Fu, *Mater. Chem. Phys*,**2009**, 115, 815.
[38] H Elmsellem, A Aouniti, M H Youssoufi, H Bendaha, T Ben hadda, A Chetouani, I Warad, BHammouti, *Phys. Chem. News* **2013**, 70, 84.
[39] F Bentiss, M Lebrini, M Lagrenee, *Corros. Sci*,**2005**, 47, 2915.
[40] T Szauer, A Brandt, *Electrochim Acta*, **1981**, 26, 1253.
[41] M Sahin, S Bilgic, H Yilmaz, *Appl. Surf. Sci*, **2002**, 195, 1.
[42] M Kissi, M Bouklah, B Hammouti, M Benkaddour, *Appl. Surf. Sci*, **2006**, 252, 4190.
[43] E Machnikova, K H Whitmire, N Hackerman, *Electrochim.Acta*, **2008**, 53, 6024.
[44] O Olivares, N V Likhanova, B Gomez, J Navarrete, M E Llanos-Serrano, E Arce, J M Hallen, *Appl. Surf. Sci*, **2006**, 252, 2894.
[45] F M Donahue, K Nobe, *J. Electrochem. Soc*, **1965**, 112, 886.
[46] A Stoyanova, G Petkova, S D Peyrimhoff, *Chem. Phys*,**2002**, 279, 1
[47] E Kamis, F Bellucci, R M Latanision, E S H El-Ashry, *Corrosion*, **1991**, 47, 677.
[48] M Ozcan, R Solmaz, G Kardas, I Dehri, *Colloid Surf.* A, **2008**, 325, 57.